



Deposited via The University of Leeds.

White Rose Research Online URL for this paper:

<https://eprints.whiterose.ac.uk/id/eprint/87065/>

Article:

Littlewood, JL, Shaw, S, Bots, P et al. (2015) Effect of solution composition on the recrystallisation of kaolinite to feldspathoids in hyperalkaline conditions: Limitations of pertechnetate incorporation by ion competition effects. *Mineralogical Magazine*, 79 (6). pp. 1379-1388. ISSN: 0026-461X

<https://doi.org/10.1180/minmag.2015.079.6.13>

Reuse

Items deposited in White Rose Research Online are protected by copyright, with all rights reserved unless indicated otherwise. They may be downloaded and/or printed for private study, or other acts as permitted by national copyright laws. The publisher or other rights holders may allow further reproduction and re-use of the full text version. This is indicated by the licence information on the White Rose Research Online record for the item.

Takedown

If you consider content in White Rose Research Online to be in breach of UK law, please notify us by emailing eprints@whiterose.ac.uk including the URL of the record and the reason for the withdrawal request.

1 Effect of solution composition on the recrystallisation of
2 kaolinite to feldspathoids in hyperalkaline conditions:
3 Limitations of pertechnetate incorporation by ion
4 competition effects.

5
6 Janice Littlewood¹, Samuel Shaw², Pieter Bots², Caroline L. Peacock¹, Divyesh Trivedi³ and Ian T.
7 Burke^{1*}

8
9 ¹ Earth Surface Science Institute, School of Earth and Environment, University of Leeds, Leeds, LS2
10 9JT, UK.

11
12 ² School of Earth, Atmospheric and Environmental Sciences, University of Manchester, Manchester,
13 M13 9PL.

14
15 ³ National Nuclear Laboratories, Risley, Warrington, Cheshire, WA3 6AS, UK.

16
17 Corresponding Author's email: i.t.burke@leeds.ac.uk

18

19 Abstract

20 The incorporation of pertechnetate (TcO_4^-) into feldspathoids produced by alkaline
21 alteration of aluminosilicate clays may offer a potential treatment route for ^{99}Tc
22 containing groundwater and liquors. Kaolinite was aged in NaOH to determine the
23 effect of base concentration, temperature, and solution composition on mineral
24 transformation and pertechnetate uptake. In all reactions, increased temperature
25 and NaOH concentration increased the rate of kaolinite transformation to
26 feldspathoid phases. In reactions containing only NaOH, sodalite was the dominant
27 alteration product however, small amounts (6-15%) of cancrinite also formed. In
28 experiments containing NaOH/Cl and NaOH/ NO_3 mixtures, sodalite and nitrate
29 cancrinite were crystallised (at 70 °C), with no reaction intermediates. The addition
30 of SO_4^{2-} crystallised sulfatic sodalite at 40 & 50 °C, but at higher temperatures (60
31 and 70 °C) sulfatic sodalite transforms to vishnevite (sulfatic cancrinite). In
32 experiments where a pertechnetate tracer was added (at $\sim 1.5 \mu\text{mol L}^{-1}$), only 3-5 %
33 of the ^{99}Tc was incorporated to the feldspathoid phases. This suggests that the
34 larger pertechnetate anion was unable to compete as favourably for the internal
35 vacancies with the smaller OH^- , NO_3^- , SO_4^{2-} or Cl^- anions in solution, making this
36 method likely to be unsuitable for groundwater treatment.

37

38 Introduction

39 There is a global legacy of contaminated land around nuclear facilities, specifically
40 arising from leaking storage ponds and containers (Mon et al., 2005, Perdril et al.,
41 2011, Wang and Um, 2012). At the Sellafield nuclear facility, UK, approximately 20
42 million m³ of soil may be contaminated, and ⁹⁰Sr, ¹³⁷Cs and ⁹⁹Tc have been identified
43 as important contaminants (Hunter, 2004). In oxic environments, technetium is
44 highly mobile in the form of its pertechnetate anion, TcO₄⁻ (Burke et al., 2005), and its
45 half-life of 2.1 x 10⁵ years (Szecsody et al., 2014) means that ⁹⁹Tc is particularly
46 problematic. Hence there is a need for low cost, preferably non-invasive, techniques
47 to be developed that might increase the pace of restoration at nuclear sites.

48 Kaolinite (Al₂Si₂O₅(OH)₄, (Grim, 1968) is commonly found in sediments and soils
49 around nuclear sites (Huertas et al., 1999), and has a simple 1:1 sheet silicate
50 structure (Bauer et al., 1998). Under alkaline conditions, kaolinite dissolves,
51 releasing Al³⁺ and Si⁴⁺ into solution, leading to the formation of secondary
52 feldspathoid and zeolite phases (Mashal et al., 2004, Qafoku et al., 2003, Zhao et
53 al., 2004, Wallace et al., 2013). The exact phase precipitated depends on the
54 solution composition, base concentration, Si:Al ratio and temperature (Deng et al.,
55 2006b). Important features of the internal structure of these neo-formed minerals,
56 such as cancrinite ((Ca,Na)₆(CO₃)_{1-1.7})[Na₂(H₂O)₂][Si₆Al₆O₂₄]) (Bonaccorsi, 2005),
57 sodalite ((Na₈Cl₂)[Si₆Al₆O₂₄]) (Bonaccorsi, 2005) and vishnevite
58 (([Na,Ca]_{6-x}K_x(SO₄))[Na₂(H₂O)₂][Si₆Al₆O₂₄]) (Bonaccorsi, 2005), are channels and
59 cages, which are known to selectively incorporate guest anions/cations (Deng et al.,
60 2006b, Mon et al., 2005). Alkaline altered sediments are known to incorporate ⁹⁰Sr
61 and ¹³⁷Cs (Choi et al., 2005, Choi et al., 2006, Chorover et al., 2008, Deng et al.,
62 2006a, Mon et al., 2005, Wallace et al., 2013), however, there is no information

63 available regarding the successful incorporation of ^{99}Tc , in the form of pertechnetate
64 (TcO_4^-), into alkaline alteration products. Perrhenate (ReO_4^-) has been incorporated
65 into sodalite (Dickson et al., 2014, Mattigod et al., 2006) and the incorporation of this
66 negatively charged, tetrahedral anion may support the hypothesis that TcO_4^- could
67 be encapsulated into similar phases. This work investigates alkaline alteration of
68 kaolinite, particularly the effect of base concentration, temperature, and solution
69 composition during aging, with a view to encapsulating ^{99}Tc , in the form of
70 pertechnetate (TcO_4^-), into a range of neoformed phases. Thus, potentially providing
71 a novel remediation treatment for land contaminated with ^{99}Tc .

72

73 Material and Methods

74 **Materials:**

75 Two natural kaolinite samples were used as supplied; kaolinite from Fluka Chemicals
76 (Switzerland) and sample K-Ga 1b from the Clay Mineral Society (Chantilly, USA).
77 Ammonium pertechnetate was obtained from LEA-CERCA (France). All other
78 reagents (sodium hydroxide, chloride, nitrate and sulfate) were obtained from VWR
79 international (USA).

80

81 **Methods:**

82 In all instances, aerobic batch experiments were carried out in sealed 50 mL
83 polypropylene Oakridge tubes. Initial experiments suspended 0.4 g of dry kaolinite
84 (Fluka) in 20 mL of NaOH solution (0.05 M, 0.5 M, 5 M), at room temperature (RT) or
85 70 °C in a temperature controlled oven (5 M NaOH only). The same solid-to-solution
86 ratio was used in all subsequent experiments. Samples were shaken on a daily
87 basis. At intervals of 1, 7, 14 and 35 days (RT), and 7 and 10 days (70 °C), tubes

88 were removed from the oven. After cooling to RT, solid phases were extracted by
89 centrifugation, at 6000 *g* for 10 minutes. The solid phase was washed four times
90 with deionised water and dried, at room temperature, in a desiccator containing
91 Carbosorb.

92

93 **Effect of solution composition and temperature:**

94 Temperature effects were determined when 0.4g dry kaolinite (Fluka) was aged in
95 20mL 5 M NaOH, for 10 days at 40 °C, 50 °C, and 60 °C. In order to investigate the
96 effect of changing the anion composition on the alteration products formed, three
97 additional basic (5 M NaOH) solutions were used that contained either 1 M NaCl, 0.5
98 M NaNO₃ or 4 M Na₂SO₄. Kaolinite (Fluka) was aged in the NaOH/Cl solution at 70
99 °C for 10 days. Kaolinite (K-Ga 1b) was aged in the NaOH/NO₃ solution at 40 °C, 50
100 °C, and 60 °C for 14 days and in the NaOH/Na₂SO₄ solution, at 40 °C, 50 °C, 60 °C
101 and 70 °C for 10 days. Additionally, 7 day time series experiments were performed
102 at 70 °C using kaolinite (K-Ga 1b) in NaOH, and kaolinite (K-Ga 1b) in the
103 NaOH/Na₂SO₄ solution, with daily sample-sacrifice.

104

105 **Pertechnetate sorption experiments**

106 Four sets of triplicate experiment were performed where ammonium pertechnetate
107 was added at tracer concentrations (1.5 μM) to each of basic solutions described
108 above (i.e NaOH, NaOH/SO₄²⁻, NaOH/NO₃⁻ and NaOH/Cl⁻) prior to the addition of
109 kaolinite (K-Ga 1b) and incubated at 70 °C for up to 72 days. At regular intervals,
110 aqueous samples were separated by centrifugation and Tc activity determined by
111 liquid scintillation counting on a Packard TriCarb 2100TR.

112

113 **Sample characterisation:**

114 The starting material and alkaline alteration end products were analysed by a
115 number of complimentary techniques. Powder X-ray diffraction (XRD) using a
116 Bruker D8 diffractometer. Samples (50-100 mg) were mounted on silicon slides and
117 scanned between 2° and 70° 2θ . Rietveld refinement was carried out using TOPAS
118 4.2 software (Bruker) providing quantitative analysis of the crystalline phases. (For
119 the results presented in this study, the errors were $\pm 10\%$ at the 50 % level (i.e.
120 between 40-60 % present) and $\pm 1\%$ close to the limit of detection (e.g. at the 3 %
121 level there was between 2-4 % present). N_2 -specific surface area was measured
122 using the BET method, with a Micrometrics Gemini V Surface Area Analyser, with
123 samples degassed for a minimum of 19 hours, at RT, with nitrogen gas prior to
124 analysis. Electron micrographs were produced using scanning electron microscopy
125 (SEM) coupled with energy-dispersive X-ray spectroscopy (EDS) using a FEI
126 QUANTA 650 FEG environmental SEM. Samples were mounted on a carbon pad
127 and coated in platinum prior to analysis.

128

129 **Results**

130 **Preliminary investigation of alkaline alteration of kaolinite in NaOH solutions.**

131 There was no evidence of new phases in the XRD patterns (not shown) where
132 kaolinite was aged in 0.05 M and 0.5 M NaOH at room temperature for 35 days. A
133 partial phase transformation to sodalite (data not shown), occurred when kaolinite
134 was aged in 5 M NaOH, however, kaolinite peaks were still dominant at day 35.
135 XRD patterns (data not shown) for the aging of kaolinite in 5 M NaOH, at 70°C ,
136 indicated that full transformation to sodalite had occurred after 10 days. Based on

137 these results, 5 M NaOH and elevated temperatures were used in subsequent
138 experiments.

139

140 **Effect of time and temperature on the alkaline alteration of kaolinite in 5 M NaOH.**

141 Kaolinite was aged over 7 days in 5 M NaOH at 70 °C. XRD patterns (figure 1A)
142 show that the transformation from kaolinite to sodalite started after 1 day, evidenced
143 by the sharp decrease in the main kaolinite (k) peak intensities and the formation of
144 peaks from the neo-formed sodalite (s) and minor amount of cancrinite (c). Rietveld
145 analysis of the day 1 and 2 samples indicated the presence of 8 and 15 wt% of
146 cancrinite (figure 2A), respectively. By day 3, sodalite was the dominant phase, with
147 only minor kaolinite peaks visible. There was no evidence of cancrinite after day 2.
148 Throughout the next 4 days, the kaolinite peaks further reduced as the sodalite
149 peaks increased, until only minor amounts of kaolinite were visible in the XRD
150 patterns by day 7. Rietveld analysis (figure 2A) of day 7 samples quantified 81 wt%
151 sodalite and 19 wt% kaolinite. BET (figure 4) analysis indicates an initial increase,
152 from 12 to 16 m²/g, in the surface area at day 1, followed by a consistent decrease in
153 surface area up to day 6 (7-10 m²/g).

154 Rietveld analysis of XRD data from 10 days experiments at lower temperatures
155 (figure 6C) showed 80 wt% sodalite and 20 wt% kaolinite at 50 °C, and 24 wt%
156 sodalite, 70 wt% kaolinite and 6 wt% cancrinite at 40 °C. This indicates that the rate
157 of clay transformation increased with temperature.

158

159 **Effect of time and temperature on the alkaline alteration of kaolinite in 5 M NaOH + 4** 160 **M Na₂SO₄**

161 XRD patterns for kaolinite aged over 7 days, in 5 M NaOH and 4 M Na₂SO₄ at 70 °C
162 are shown in Figure 1B. We note sharp decreases in the kaolinite (k) peak intensities
163 between the starting material and the 1 day aged sample. The decrease in the
164 kaolinite peaks, and the appearance of small peaks at 13.9° and 24.4° 2θ was
165 consistent with the transformation from kaolinite to sulfatic sodalite/vishnevite.
166 Rietveld analysis (figure 2B) of the day 1 samples quantified the neofomed
167 feldspathoids as 2 wt% vishnevite and 29 wt% sodalite. After two days aging, the
168 XRD patterns (figure 1B) showed further reductions in the kaolinite peak intensities
169 (k) together with increasing sulfatic sodalite peak intensities (s). Rietveld analysis
170 (figure 2B) for the day 2 samples showed that sulfatic sodalite had increased to 62
171 wt%, vishnevite had increased to 2.5 wt% and kaolinite had decreased to 35.5 wt%.
172 By day 3, peaks for vishnevite (v) increased in intensity (figure 1B.), and only minor
173 kaolinite peaks were visible. Throughout the next four days, the kaolinite peaks
174 further reduced and the sodalite/vishnevite (s/v) peaks became more prominent until
175 only minor amounts of kaolinite were visible in the XRD patterns by day 7. After 7
176 days, Rietveld analysis (figure 2B) showed that sodalite had decreased to 24 wt%,
177 vishnevite had increased to 53 wt% and kaolinite had decreased to 23 wt%. This
178 suggested that the kaolinite transformed to vishnevite, via a sulfatic sodalite
179 intermediate phase. No broad humps were observed in the XRD patterns at any
180 time during the reaction indicating that there were no amorphous phases detected at
181 any time during the transformations.

182 SEM images (figure 3) of the solid phases collected during the transformation show
183 the kaolinite starting material and the sulfatic sodalite/vishnevite alteration product at
184 day 2 and 7. The kaolinite starting material (figure 3A) comprised multiple layers of
185 stacked hexagonal plates approximately 20-30 μm in size. The EDS spectra of

186 kaolinite showed the presence of Al, Si and O, with the Al and Si peaks present at
187 equal intensities. After 1 day of aging, the overall crystal morphology of the kaolinite
188 had evolved (data not shown). An interlocking desert rose morphology,
189 characteristic of cancrinite (Deng et al., 2006), was observed after 2 days (figure 3B).
190 These crystallites were approximately 2.5 μm in diameter and contained O, Al, Si,
191 Na, and S by EDS analysis, consistent with formation of sulfatic sodalite or
192 vishnevite. By day 7, the sample crystal morphology comprised spheres of
193 interlocking tabular crystals (figure 3C) with a diameter of $\sim 3\text{-}5\mu\text{m}$. BET (figure 4)
194 analysis indicates similar change to those observed in the pure NaOH system with
195 an initial increase (12 to 15 m^2/g) in surface area at day 1 followed by a consistent
196 decrease in surface area up to day 6 (4-6 m^2/g).

197 XRD patterns (figure 5) in respect of the aging of kaolinite in 5 M NaOH and 4 M
198 Na_2SO_4 , at 70 $^\circ\text{C}$ for 10 days, showed the presence of sulfatic sodalite and
199 vishnevite. Rietveld analysis (figure 6B) of a sample aged at 60 $^\circ\text{C}$ for 10 days
200 quantified the phases to be 34 wt% sulfatic sodalite, 8 wt% kaolinite and 58 wt%
201 vishnevite. After 10 days aging at 50 $^\circ\text{C}$ the reaction products were 69.5 wt% sulfatic
202 sodalite and 30.5 wt% kaolinite. At 40 $^\circ\text{C}$ the reaction products were 36 wt% sulfatic
203 sodalite and 64 wt%. This suggested that at lower temperatures kaolinite transforms
204 to sulfatic sodalite, and to vishnevite at higher temperatures.

205

206 **Alkaline alteration of kaolinite in 5 M NaOH + 1 M NaCl or 0.5 M NaNO_3**

207 The addition of 1 M NaCl to the 5 M NaOH solution led (figure 5) to the
208 transformation of kaolinite to sodalite after 10 days aging at 70 $^\circ\text{C}$. In contrast XRD
209 data shows that aging kaolinite in 5 M NaOH + 0.5 M NaNO_3 for 14 days at 60 $^\circ\text{C}$
210 (figure 5) led to the formation of nitrate-cancrinite. Trace amounts of kaolinite (figure

211 5) were still present after 14 days. Rietveld analysis (figure 6A) of the 14 day sample
212 quantified the phases to be 98.5 wt% nitrate-cancrinite and 1.5 wt% kaolinite, which
213 suggested that the kaolinite to nitrate-cancrinite transformation was almost complete
214 after 14 days. Experiments were also carried out at lower temperatures and showed
215 an increase in the amount of kaolinite remaining after 14 days (i.e. 8 wt% at 50 °C
216 and 31 wt% at 40 °C). This indicates that the rate of transformation from kaolinite to
217 nitrate-cancrinite increased as temperature increased, and no reaction intermediates
218 were present.

219 **Pertechnetate incorporation behaviour during phase transformation**

220 The % ⁹⁹Tc remaining in solution (figure 7) during the aging of kaolinite in either 5 M
221 NaOH, 5 M NaOH +1 M NaCl, 5 M NaOH + 0.5 M NaNO₃, or 5 M NaOH + 4 M
222 Na₂SO₄, was very high, ~ 95-97 %, in all instances. This suggested that only a small
223 uptake to solids (~ 3-5 % ⁹⁹Tc; figure 7, inset) occurred during the first 9 days of
224 aging. Although these experiments continued for 72 days, no further uptake was
225 observed.

226

227 **Discussion**

228 The end products which form during alkaline alteration of kaolinite vary depending on
229 base concentration, temperature and solution composition. The lack of mineral
230 transformation during the reaction of kaolinite in 0.05 M and 0.5 M NaOH, and partial
231 transformation to sodalite in 5 M NaOH at RT, implied that there was a threshold
232 concentration effect between 0.5 M and 5 M NaOH. Full transformation at higher
233 [NaOH] is anticipated as the increased rate of a reaction is related to increases in

234 base concentration. The rate of mineral transformation is also higher at higher
235 temperatures (Mashal and Cetiner, 2010).

236 Our experiments showed that in 5 M NaOH, kaolinite started to transform to sodalite
237 at 70 °C after 1 day, with only trace kaolinite remaining after 7 days. In previous
238 work on feldspathoid precipitation from both kaolinite (Rios et al., 2009, Zhao et al.,
239 2004) and Si-Al solutions (Deng et al., 2006b), amorphous and zeolitic intermediates
240 were observed before sodalite and cancrinite precipitation. However, we did not
241 observe these intermediate phases in our experiments.

242

243 **Effect of solution composition on alteration product formation**

244 It is thought that guest anions form ion-pairs with Na⁺ ions in solution, inducing the
245 nucleation and growth of the neoformed feldspathoid end-products (Zhao et al.,
246 2004). As we have stated, the end products vary depending on which anions are
247 present in solution (Choi et al., 2006), and incorporation of guest ions is likely to be
248 size dependent. The anion-Na⁺ ion pairs must be able to fit inside the cages and
249 channels of the aluminosilicate minerals which grow around them (Barrer et al.,
250 1968). In this study, the addition of sodium sulfate, sodium nitrate and sodium
251 chloride produced end products of sulfatic sodalite/vishnevite ($[(\text{Na,Ca})_6\text{-}$
252 $x\text{K}_x(\text{SO}_4)][\text{Na}_2(\text{H}_2\text{O})_2][\text{Si}_6\text{Al}_6\text{O}_{24}]$), nitrate-cancrinite ($\text{Na}_6[\text{Si}_6\text{Al}_6\text{O}_{24}] \cdot 2\text{NaNO}_3$) and
253 sodalite ($(\text{Na}_8\text{Cl}_2)[\text{Si}_6\text{Al}_6\text{O}_{24}]$), respectively. The formation of nitrate cancrinite and
254 vishnevite resulted in guest anion substitution of NO₃⁻ and SO₄²⁻ into the ideal
255 cancrinite structure. The sodalite structure does not have the wide channels found in
256 cancrinite, only cages. These cages contain a central anion, tetrahedrally bound to
257 four cations. As the ideal sodalite structure has a central Cl⁻ anion, the formation of

258 sodalite in the presence of sodium chloride is as anticipated (Barrer et al., 1974),
259 (Zhao et al., 2004).

260 In the NaOH/NO₃⁻ system no reaction intermediates were observed for the
261 transformation of kaolinite to nitrate cancrinite (figure 5). The formation of nitrate
262 cancrinite in high NO₃⁻ experiments has been previously reported (Buhl et al., 2000,
263 Zhao et al., 2004). In our experiments, the degree of reaction for the NaOH/NO₃⁻
264 system was more than any of the other systems tested, with 69, 92 and 98 wt%
265 transformation from kaolinite to nitrate-cancrinite at temperatures of 40, 50 & 60 °C
266 after 14 days.

267

268 **Reaction pathway for the NaOH/SO₄²⁻ system**

269 The transformation of kaolinite aged in NaOH/SO₄²⁻ has not been reported
270 previously, therefore, this reaction pathway was studied in more detail. The XRD
271 patterns (figure 1B) observed for the alteration products are similar to those for
272 sulfate-cancrinite which was synthesised from aluminosilicate solutions (Deng et al.,
273 2006b). The morphological changes, observed via SEM (figure 3), show blade-like
274 spheres at day 2 which are similar to those which have been reported in the
275 literature for cancrinite (Choi et al., 2005), however that reaction was performed at a
276 lower base concentration, (0.01 M NaOH instead of 5 M) and for a longer time period
277 (190 days compared to 7 days). The appearance of peaks for Na and for S in SEM-
278 EDS analysis, which were not present in the starting material, support the formation
279 of sulfatic sodalite/vishnevite. In summary, XRD, SEM, EDS and surface area
280 evidence all suggest that the partial alkaline alteration of kaolinite started after 1 day
281 of reaction.

282 Vishnevite (sulfate cancrinite) formation was observed after 3 days of reaction.
283 Rietveld analysis (figure 6B) shows a gradual increase in the % vishnevite over days
284 4 to 7, to 53 %, with the amount of sulfatic sodalite decreasing to 24 % over the
285 same period. This is consistent with the dissolution of sulfatic sodalite and the
286 crystallisation of vishnevite. SEM images of the reaction products at day 7 (figure
287 3c) showed minor changes in morphology, in that the spheres were smaller and
288 more tabulated, which is similar to other SEM images reported for cancrinite (Deng
289 et al., 2006c). The smaller size of the day 7 spheres was reflected by a slight
290 increase in the surface area indicating some dissolution of sodalite and
291 recrystallisation to vishnevite. By 7 days 78 % of the original kaolinite had reacted
292 producing vishnevite at 70 °C (via a sulfatic sodalite intermediate). The sodalite
293 intermediate is more stable at lower temperatures evidenced by the lack of
294 vishnevite at 40 and 50 °C.

295

296 **Proposed incorporation of ⁹⁹Tc into alkaline altered clays**

297 The potential incorporation of the technetium anion, pertechnetate (TcO_4^-), into
298 cancrinite or sodalite has received some support from other authors (Mattigod et al.,
299 2006, Dickson et al., 2014); however, the successful incorporation of technetium into
300 feldspathoids has not yet been achieved. The results (figure 7) of the low
301 concentration pertechnetate experiments showed only a very small ⁹⁹Tc uptake
302 under any of the reaction conditions studied. Up to 5 % sorption of ⁹⁹Tc to alkaline
303 alteration products was observed in all instances. Using sulfate to drive the reaction
304 toward sulfate cancrinite did not produce any increased uptake over other anions
305 such as chloride or nitrate (despite the analogous tetrahedral coordination of SO_4^{2-}
306 and TcO_4^-). TcO_4^- is a relatively large anion (~2.5 Å), and in cancrinite ⁹⁹Tc is likely

307 to have been incorporated into a channel rather than a cage due to size constraints.
308 Sodalite does not have channels, so the incorporation of ^{99}Tc would have been into
309 the cages. The low ^{99}Tc uptake could suggest that the large pertechnetate anion is
310 unable to compete favourably for the internal sites with the smaller, and therefore
311 more size appropriate, OH^- , Cl^- , NO_3^- , or SO_4^{2-} anions (~ 1.4 , ~ 1.7 , ~ 2.0 and ~ 2.3 Å
312 respectively), at these low concentrations. The successful incorporation of ^{99}Tc into
313 alkaline alteration end products such as cancrinite and sodalite could provide a
314 substantial research contribution. However, very high concentrations of
315 pertechnetate (and conversely low concentrations of other anions) are likely to be
316 required to produce significant uptake of ^{99}Tc to alkaline alteration end products.

317

318 Conclusions

319 Kaolinite undergoes alkaline alteration in the presence of 5 M NaOH (both with and
320 without Cl^-) at 70 °C to sodalite, to vishnevite if sulfate is present (via sulfatic sodalite
321 at lower temperatures), and to nitrate cancrinite in the presence of nitrate. The rate
322 of reaction was faster for the OH and OH/ NO_3^- systems relative to the OH/ SO_4^{2-}
323 system. Up to 5 % ^{99}Tc tracer could be incorporated into these alkaline altered
324 feldspathoids which is insufficient to consider alkaline alteration of clay minerals to
325 be a remediation strategy for ^{99}Tc .

326

327

329 BARRER, R. M., BEAUMONT, R. & COLLELA, C. 1974. CHEMISTRY OF SOIL
330 MINERALS .14. ACTION OF SOME BASIC SOLUTIONS ON
331 METAKAOLINITE AND KAOLINITE. *Journal of the Chemical Society-Dalton*
332 *Transactions*, 934-&.

333 BARRER, R. M., COLE, J. F. & STICHER, H. 1968. CHEMISTRY OF SOIL MINERALS
334 .5. LOW TEMPERATURE HYDROTHERMAL TRANSFORMATIONS OF
335 KAOLINITE. *Journal of the Chemical Society a -Inorganic Physical Theoretical*,
336 2475-&.

337 BAUER, A., VELDE, B. & BERGER, G. 1998. Kaolinite transformation in high molar KOH
338 solutions. *Applied Geochemistry*, 13, 619-629.

339 BONACCORSI, E., MERLINO., S 2005. Modular Microporous Minerals: Cancrinte-Dayne
340 Group and C-S-H Phases. *Reviews in Mineralogy & Geochemistry*, 57, 241-290.

341 BUHL, J. C., STIEF, F., FECHTELKORD, M., GESING, T. M., TAPHORN, U. & TAAKE,
342 C. 2000. Synthesis, X-ray diffraction and MAS NMR characteristics of nitrate
343 cancrinite Na-7.6 AlSiO₄ (6)(NO₃)(1.6)(H₂O)(2). *Journal of Alloys and Compounds*,
344 305, 93-102.

345 BURKE, I. T., BOOTHMAN, C., LLOYD, J. R., MORTIMER, R. J. G., LIVENS, F. R. &
346 MORRIS, K. 2005. Effects of progressive anoxia on the solubility of technetium in
347 sediments. *Environmental Science & Technology*, 39, 4109-4116.

348 CHOI, S., CROSSON, G., MUELLER, K. T., SERAPHIN, S. & CHOROVER, J. 2005. Clay
349 mineral weathering and contaminant dynamics in a caustic aqueous system - II.
350 Mineral transformation and microscale partitioning. *Geochimica Et Cosmochimica*
351 *Acta*, 69, 4437-4451.

352 CHOI, S., O'DAY, P. A., RIVERA, N. A., MUELLER, K. T., VAIRAVAMURTHY, M. A.,
353 SERAPHIN, S. & CHOROVER, J. 2006. Strontium speciation during reaction of
354 kaolinite with simulated tank-waste leachate: Bulk and microfocused EXAFS
355 analysis. *Environmental Science & Technology*, 40, 2608-2614.

356 CHOROVER, J., CHOI, S., ROTENBERG, P., SERNE, R. J., RIVERA, N., STREPKA, C.,
357 THOMPSON, A., MUELLER, K. T. & O'DAY, P. A. 2008. Silicon control of
358 strontium and cesium partitioning in hydroxide-weathered sediments. *Geochimica Et*
359 *Cosmochimica Acta*, 72, 2024-2047.

360 DENG, Y., FLURY, M., HARSH, J. B., FELMY, A. R. & QAFOKU, O. 2006a. Cancrinite
361 and sodalite formation in the presence of cesium, potassium, magnesium, calcium and
362 strontium in Hanford tank waste simulants. *Applied Geochemistry*, 21, 2049-2063.

363 DENG, Y., HARSH, J. B., FLURY, M., YOUNG, J. S. & BOYLE, J. S. 2006b. Mineral
364 formation during simulated leaks of Hanford waste tanks. *Applied Geochemistry*, 21,
365 1392-1409.

366 DENG, Y. J., FLURY, M., HARSH, J. B., FELMY, A. R. & QAFOKU, O. 2006c. Cancrinite
367 and sodalite formation in the presence of cesium, potassium, magnesium, calcium and
368 strontium in Hanford tank waste simulants. *Applied Geochemistry*, 21, 2049-2063.

369 DICKSON, J. O., HARSH, J. B., FLURY, M., LUKENS, W. W. & M., P. E. 2014.
370 Competitive Incorporation of Perrhenate and Nitrate into Sodalite. *Environ. Sci.*
371 *Technol*, DOI: 10.1021/es503156v.

372 GRIM, R. E. (ed.) 1968. *Clay Mineralogy*.

373 HUERTAS, F. J., CHOU, L. & WOLLAST, R. 1999. Mechanism of kaolinite dissolution at
374 room temperature and pressure Part II: Kinetic study. *Geochimica Et Cosmochimica*
375 *Acta*, 63, 3261-3275.

376 HUNTER, J. 2004. SCLS Phase 1 - Conceptual model of contamination below ground at
377 Sellafield, BNFL.

378 MASHAL, K., HARSH, J. B., FLURY, M., FELMY, A. R. & ZHAO, H. T. 2004. Colloid
379 formation in Hanford sediments reacted with simulated tank waste. *Environmental*
380 *Science & Technology*, 38, 5750-5756.

381 MASHAL, K. Y. & CETINER, Z. S. 2010. Experimental investigation of cesium mobility in
382 the course of secondary mineral formations in Hanford sediment columns at 50
383 degrees C. *Environmental Monitoring and Assessment*, 169, 249-258.

384 MATTIGOD, S. V., MCGRAIL, B. P., MCCREAD, D. E., WANG, L. Q., PARKER, K. E.
385 & YOUNG, J. S. 2006. Synthesis and structure of perrhenate sodalite. *Microporous*
386 *and Mesoporous Materials*, 91, 139-144.

387 MON, J., DENG, Y. J., FLURY, M. & HARSH, J. B. 2005. Cesium incorporation and
388 diffusion in cancrinite, sodalite, zeolite, and allophane. *Microporous and Mesoporous*
389 *Materials*, 86, 277-286.

390 PERDRIAL, N., RIVERA, N., THOMPSON, A., O'DAY, P. A. & CHOROVER, J. 2011.
391 Trace contaminant concentration affects mineral transformation and pollutant fate in
392 hydroxide-weathered Hanford sediments. *Journal of Hazardous Materials*, 197, 119-
393 127.

394 QAFOKU, N. P., AINSWORTH, C. C., SZECSDY, J. E. & QAFOKU, O. S. 2003.
395 Aluminum effect on dissolution and precipitation under hyperalkaline conditions: I.
396 Liquid phase transformations. *Journal of Environmental Quality*, 32, 2354-2363.

397 RIOS, C. A., WILLIAMS, C. D. & FULLEN, M. A. 2009. Nucleation and growth history of
398 zeolite LTA synthesized from kaolinite by two different methods. *Applied Clay*
399 *Science*, 42, 446-454.

400 SZECSDY, J. E., JANSIK, D. P., MCKINLEY, J. P. & HESS, N. J. 2014. Influence of
401 alkaline co-contaminants on technetium mobility in vadose zone sediments. *Journal*
402 *of Environmental Radioactivity*, 135, 147-160.

403 WALLACE, S. H., SHAW, S., MORRIS, K., SMALL, J. S. & BURKE, I. T. 2013.
404 Alteration of Sediments by Hyperalkaline K-Rich Cement Leachate: Implications for
405 Strontium Adsorption and Incorporation. *Environmental Science & Technology*, 47,
406 3694-3700.

407 WANG, G. & UM, W. 2012. Mineral dissolution and secondary precipitation on quartz sand
408 in simulated Hanford tank solutions affecting subsurface porosity. *Journal of*
409 *Hydrology*, 472, 159-168.

410 ZHAO, H. T., DENG, Y. J., HARSH, J. B., FLURY, M. & BOYLE, J. S. 2004. Alteration of
411 kaolinite to cancrinite and sodalite by simulated hanford tank waste and its impact on
412 cesium retention. *Clays and Clay Minerals*, 52, 1-13.

413
414

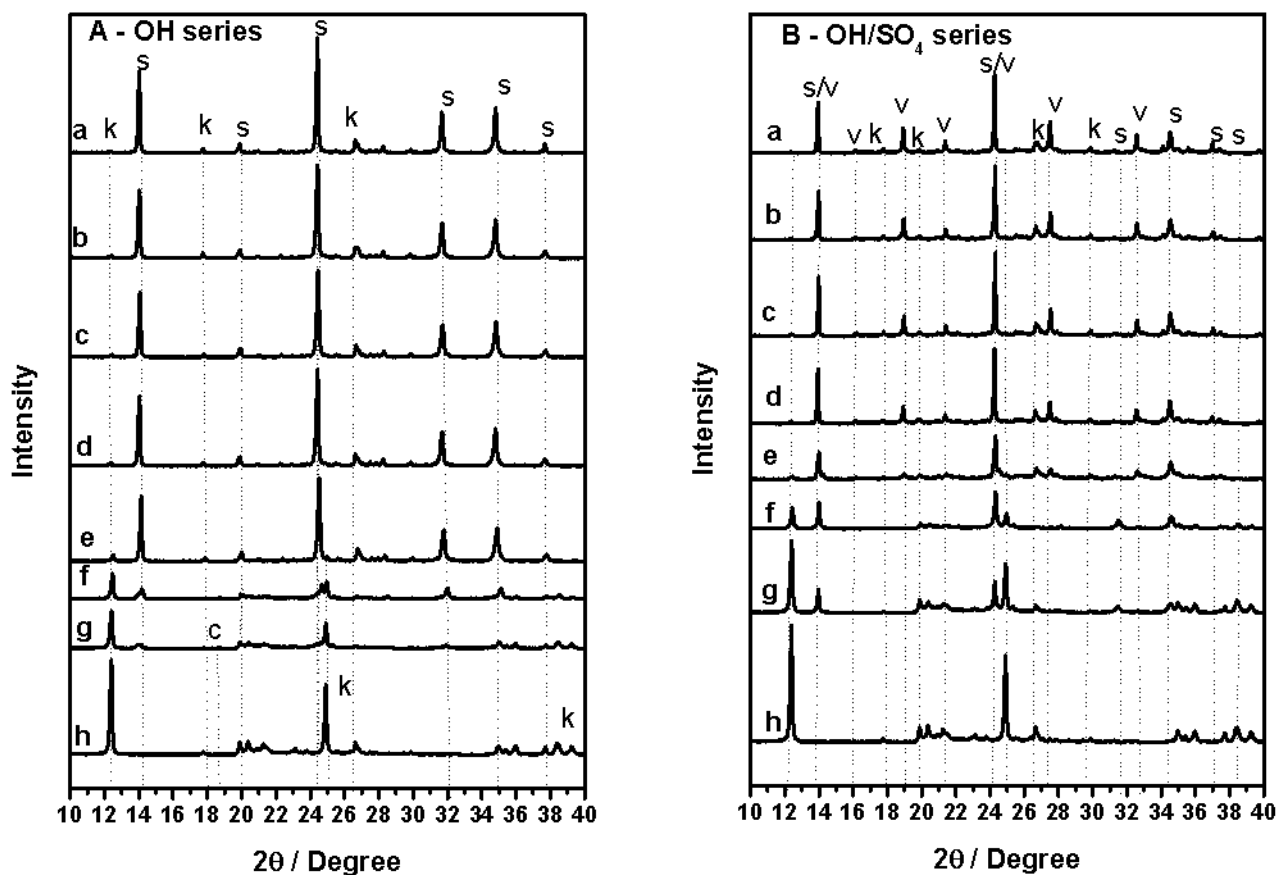


Figure 1: X-ray diffraction (XRD) patterns of kaolinite aged in 5M NaOH (A) and 5M NaOH/SO₄ (B) at 70°C for a) 7 days, b) 6 days, c) 5 days, d) 4 days, e) 3 days, f) 2 days & g) 1 day. The XRD pattern of the kaolinite starting material is shown in h). Minerals are annotated as s (sodalite), k (kaolinite), v (vishnevite) and c (cancrinite).

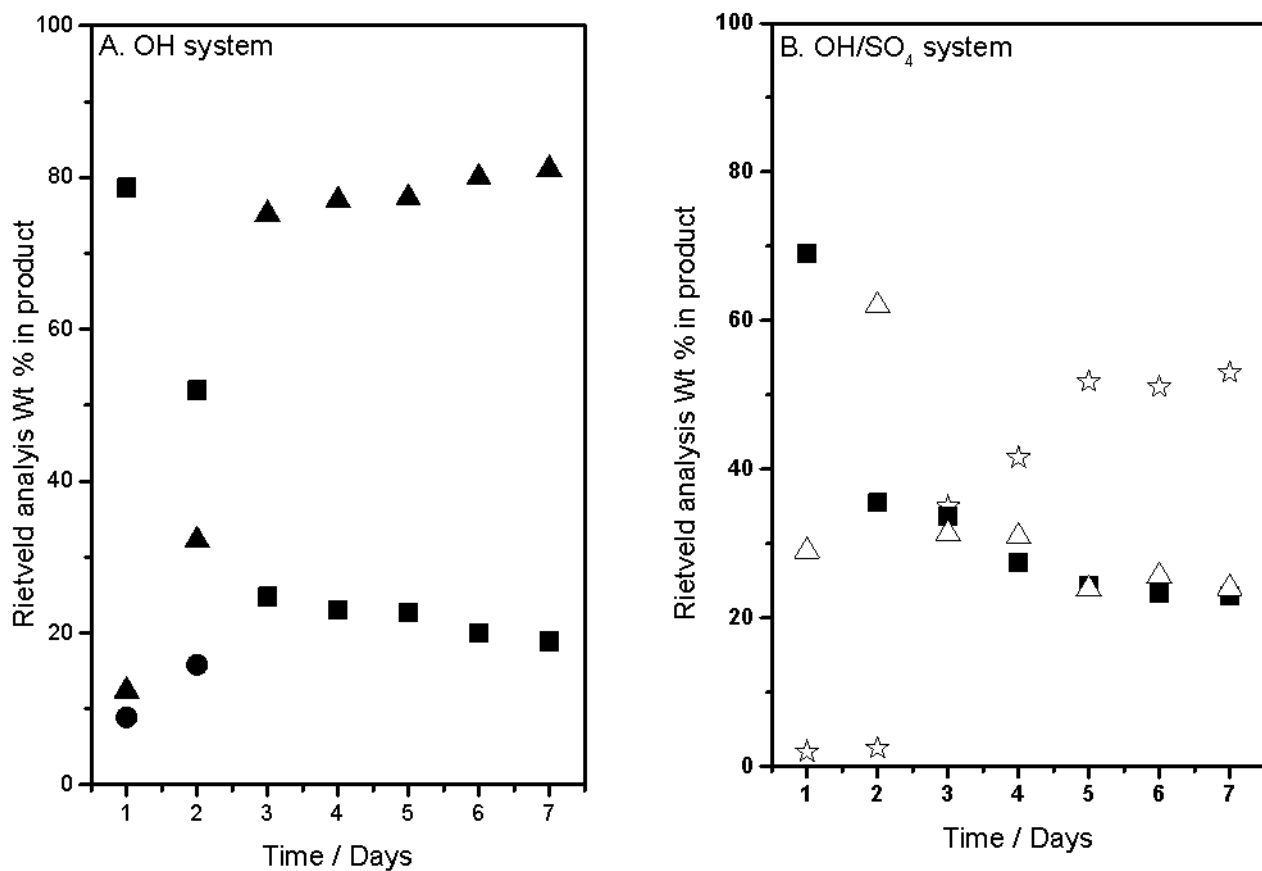


Figure 2: Rietveld analysis for kaolinite aged in 5M NaOH (A) and 5M NaOH/SO₄ (B) at 70°C for 7 days. Mineral Wt % are shown for kaolinite (squares), sodalite (triangles), cancrinite (circles) and vishnevite (stars). Muscovite impurity in the starting material not shown.

420

421

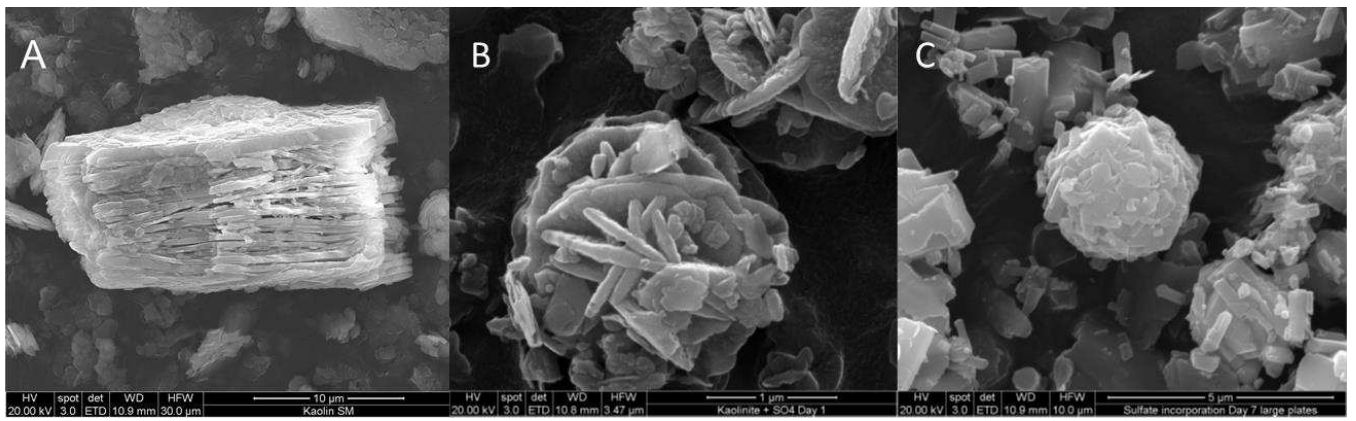


Figure 3: SEM images for kaolinite A) and the alkaline alteration product formed during the aging of kaolinite in 5M NaOH + SO₄ (4M) at 70°C for B) 2 days & C) 7 days.

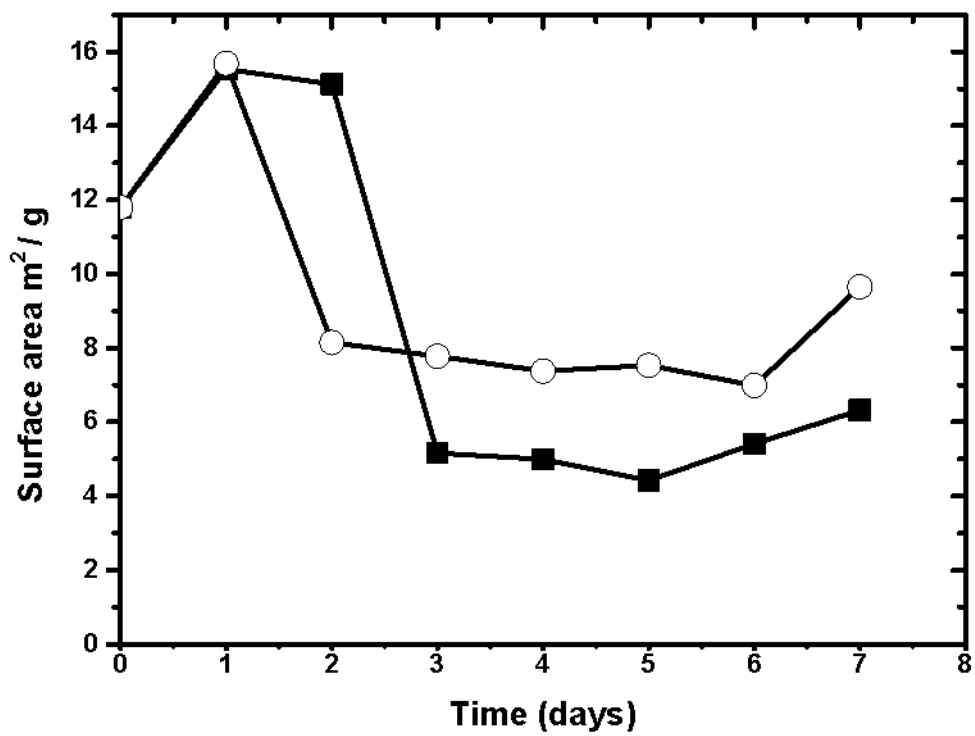


Figure 4: Changes in mineral surface area during the reaction of kaolinite in 5M NaOH (circles) and NaOH/SO₄ (squares) at 70°C for 7 days.

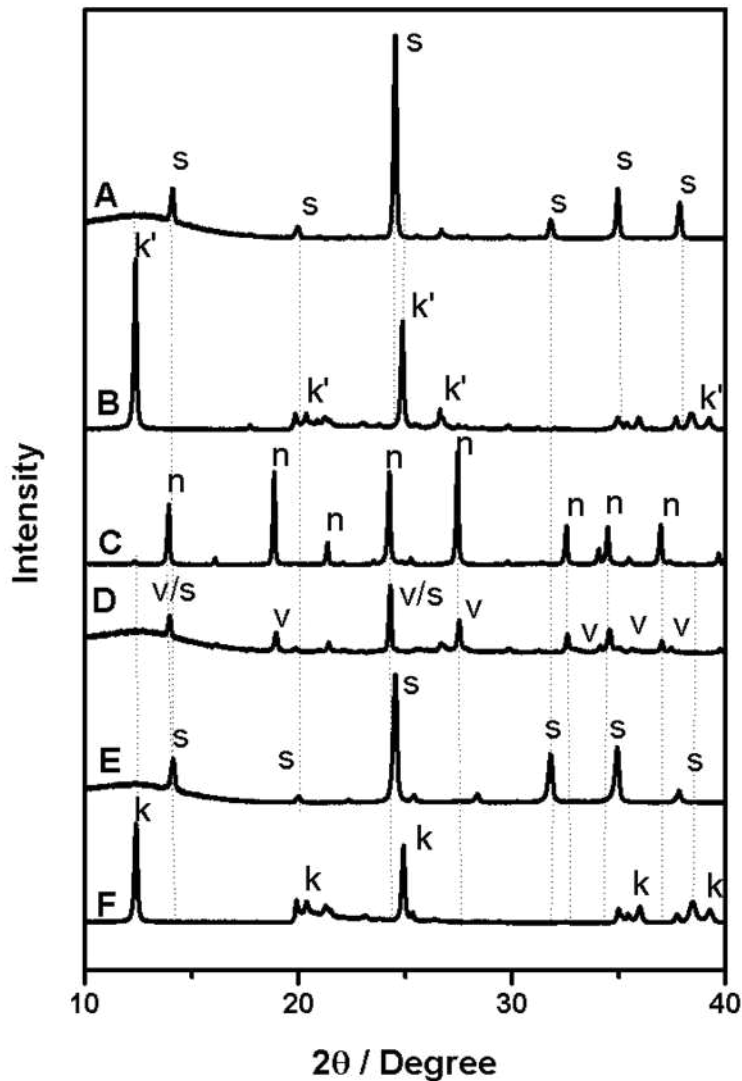


Figure 5: XRD patterns of (A) sodalite, annotated as s, the alkaline alteration product of (B) kaolinite (Fluka), annotated as k', aged in 5M NaOH + Cl at 70 °C for 10 day; (C) nitrate cancrinite, annotated as n, the alkaline alteration product of (F) kaolinite (K-Ga 1b), annotated as k reacted in 5M NaOH + NO₃ (60 °C, 14 days); (D) sulfatic sodalite/vishnevite, annotated as s/v the alkaline alteration product of (F) kaolinite (K-Ga 1b), annotated as k reacted in 5M NaOH + SO₄ (70 °C, 10 days) and (E) sodalite, annotated as s, the alkaline alteration product of (F) kaolinite (K-Ga 1b), annotated as k reacted in 5M NaOH (70 °C, 10 days).

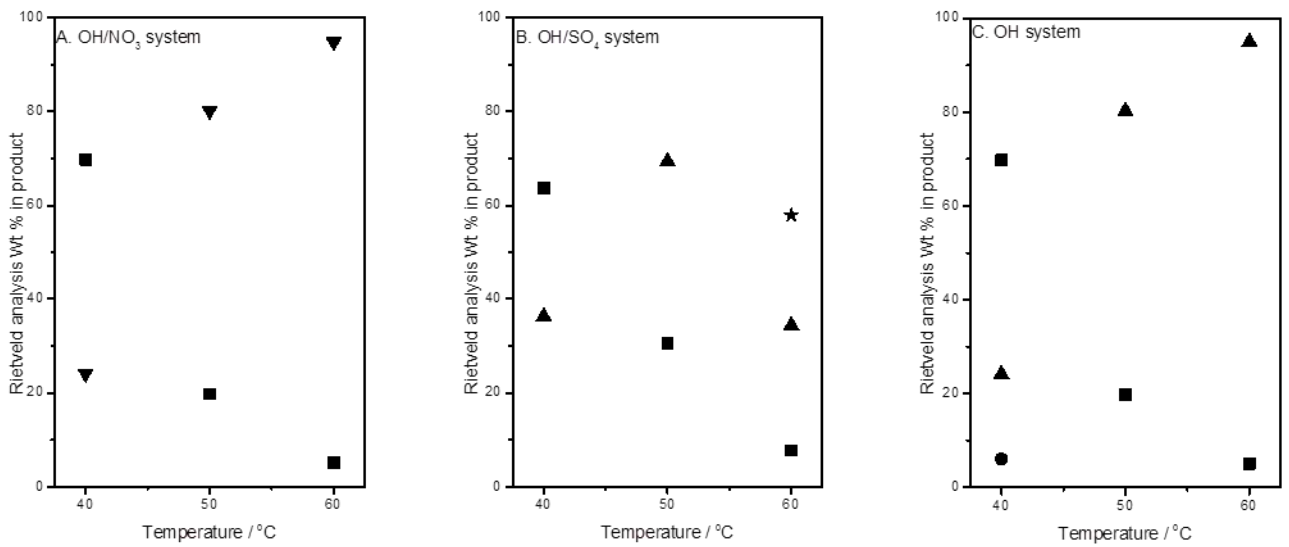


Figure 6: Rietveld analysis for kaolinite aged in A) 5M NaOH + NO₃ for 14 days at 40,50 & 60°C. Mineral Wt % are shown for kaolinite (squares) and nitrate cancrinite (inverted triangles), in B) 5M NaOH + SO₄ for 10 days at 40,50 & 60°C. Mineral Wt % are shown for kaolinite (squares), sulfatic sodalite (triangles) and vishnevite (stars) and in C) 5M NaOH for 10 days at 40,50 & 60°C. Mineral Wt % are shown for kaolinite (squares), sodalite (triangles) and cancrinite (circles).

433

434

435

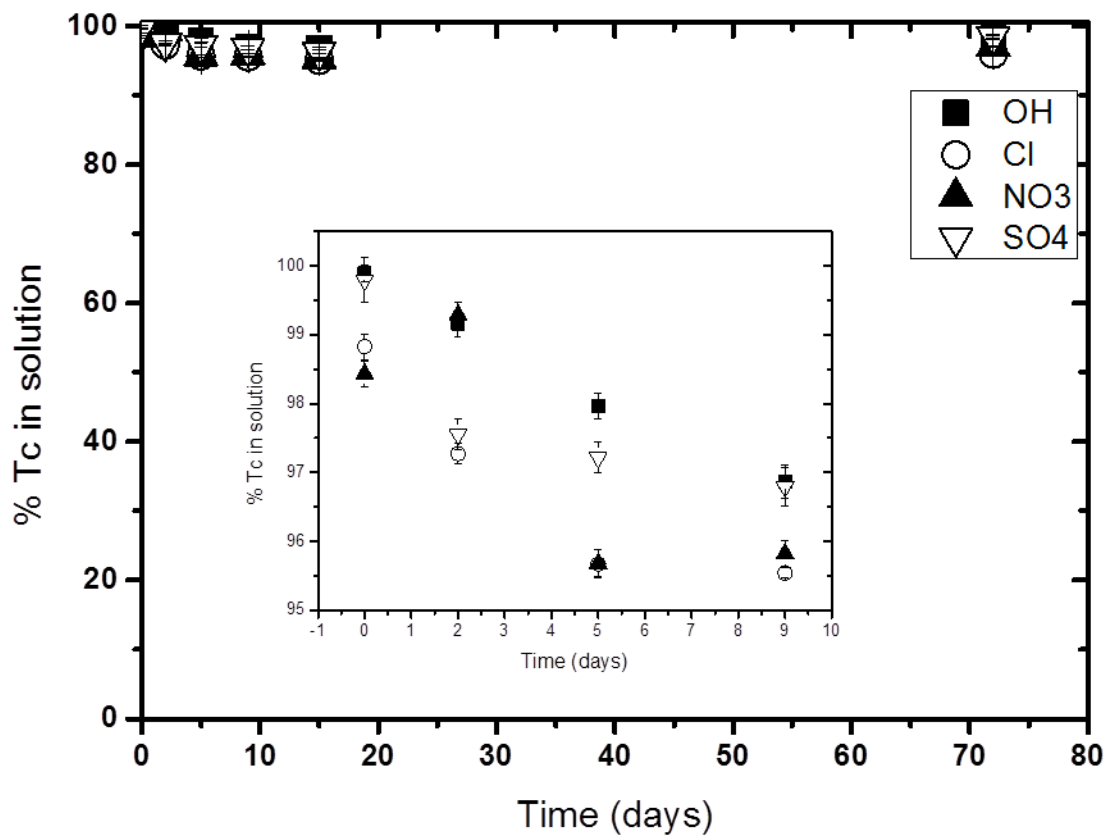


Figure 7: % ⁹⁹Tc (30 Bq/mL spike) in solution after aging kaolinite in 5M NaOH (squares), 5M NaOH plus Cl (circles), 5M NaOH plus NO₃ (triangles) and 5M NaOH plus SO₄ (inverted triangles) at 70°C for 72 days.

436
437